A New Heat Flux Sensor: From Microvolts to Millivolts

Vital M. Meyer and Bruno Keller

Chair of Building Physics,
Institute of Building Technologies,
ETH Hönggerberg, CH-8093 Zurich, Switzerland

A newly developed heat flux sensor of very high sensitivity is presented. It is based on the well-known Seebeck effect. We made use of the technique of anisotropic silicon etching, the thermoelectric material properties of Bi/Sb and the photolithography used for microelectronics. The resulting sensor has a sensitivity of about $10 \text{ mV·m}^2 / \text{W}$ which corresponds to a responsivity of about 20 V/W. This is higher by a factor of about 100 than that of the best commercially available heat flux sensors.

1.   Introduction

Heat flux measurements are of interest in various fields: in some applications, like calorimetric measurement of specific heat, melting heat etc., the integral of the heat flux over time is of primary interest.

In building physics, we are interested in the heat flux density, *e.g.* as a criterion of a wall construction under steady state thermal conditions. In real-world buildings, however, steady state thermal conditions are never reached. The shortwave radiation of the sun, stochastic changes of external temperatures and internal heat sources, rapidly changing air flux patterns, etc., influence the thermal behavior of a room. In such a complex thermal environment, it is necessary to measure the heat fluxes directly instead of measuring temperatures and calculating heat fluxes by the use of more or less well-known thermal film coefficients.

The main reason why there are so few heat flux measurements is the poor behavior of the commercially available heat flux sensors. They tend to be thick and thus have high thermal resistance. Moreover, the signal density (signal per active area) is low. This makes it impossible to perform measurements with high spatial resolution.

2.   Design of Conventional Heat Flux Sensors

Most heat flux sensors[1–4] consist of a thin layer of material (rubber, plastic) in which a thermopile is encapsulated (see Fig. 1). A heat flux perpendicular to the substrate induces a small temperature difference $\Delta\vartheta$ over each thermocouple. These temperature differences are summed by a number of thermocouples connected in parallel thermally and in series electrically. In this manner, we measure an integral heat flux signal over the sensor area.

All existing heat flux sensors have one or more serious drawbacks:
— large substrate thickness and therefore high thermal resistance disturbs the heat flux measured
— the intrinsic three-dimensional structure of the thermopile complicates production and is prohibitive for microtechnological structuring methods
— the use of wires severely restricts the choice of thermoelectric materials

3.   New Design

3.1 *Design criteria*
Our aims for the new sensor design were the following.
— maximizing the sensitivity of the sensor
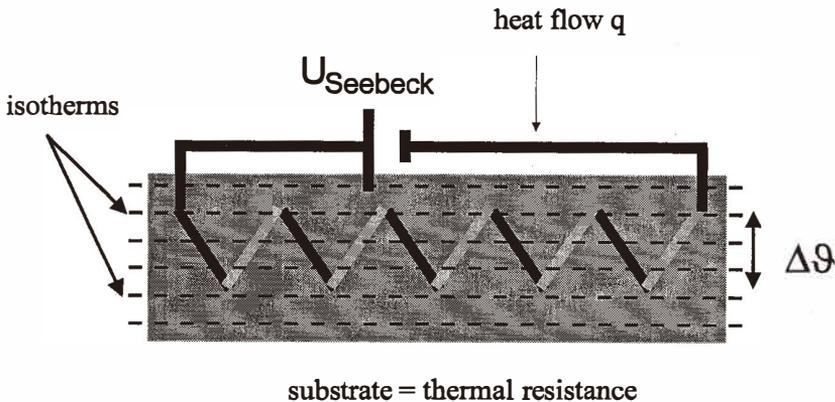— minimizing the thermal resistance of the sensor

Fig. 1.   Conventional heat flux sensor.

— physical thickness of the sensor less than 1 mm
— sufficient robustness of the design
— low production costs

3.2 *Sensitivity of the sensor*

The output signal U of a heat flux sensor is a dc-voltage. In a linear approximation:

$$U = N \cdot \alpha_{pn} \cdot \Delta \vartheta \tag{1}$$

where N: number of thermocouples, α_{pn}: Seebeck coefficient between the positive and the negative thermoelectric materials and $\Delta \vartheta$: temperature difference over the thermocouples (see Fig. 1). $\Delta \vartheta$ is proportional to the heat flux:

$$\Delta \vartheta = R_{th} \cdot q \tag{2}$$

where R_{th} [K·m²/W]: effective thermal resistance of substrate and thermocouple and q [W/m²]: heat flux.

To characterize a heat flux sensor, we have to distinguish between two important quantities. First, the sensitivity S [V·m²/W] is the output voltage per unit of heat flux:

$$S = \frac{U}{q} = N \cdot \alpha_{pn} \cdot R_{th} = n \cdot A_{Sensor} \cdot \alpha_{pn} \cdot R_{th} \tag{3}$$

where n is the density of thermocouples per active area A_{sensor} (the sensitive area of the sensor). This quantity is usually given in the heat flux sensor literature. Another very important quantity is the responsivity $\mathcal{R}$ [V/W] which is simply the sensitivity divided by the active area of the sensor:

$$\mathcal{R} = \frac{S}{A_{Sensor}} = n \cdot \alpha_{pn} \cdot R_{th} \,. \tag{4}$$

With sensors of high responsivity, measurements are possible with a small active area A_{sensor} and therefore with high spatial resolution.

To express the efficiency of a heat flux sensor in terms of measurements we are interested in, we define a "quality number" Q:

$$Q = \frac{\mathcal{R}^2}{d_s \cdot R_{th}} \tag{5}$$

where d_s: thickness of the sensor. The quality number takes into account not only the

responsivity but also the effective thermal resistance and the thickness of the sensor which disturbs the heat flux.

3.3   *The material: figures of merit and noise*

In order to select the best thermoelectric materials for our purpose, we consider the signal-to-noise ratio of our sensor. The noise U_{ns} of a thermopile is mainly thermal noise and determined by its internal resistance R. It is given by the well-known Johnson formula:

$$U_{ns} = \sqrt{4 \cdot k \cdot T \cdot R \cdot \Delta f} \qquad (6)$$

where k: Boltzmann constant, R: electrical resistance of the thermopile and Δf: frequency bandwidth.

Assuming a thermopile with N thermocouples composed of two equal legs with dimensions l, A_{TC} (length of thermocouple leg, thermocouple cross section) with resistivity ρ_p, ρ_n, respectively, the internal resistance is equal to

$$
\begin{aligned}
R &= N \cdot \frac{l}{A_{TC}} \cdot (\rho_p + \rho_n) \\
  &= N \cdot \frac{l}{A_{TC}} \cdot \rho_{sum}
\end{aligned}
\qquad (7)
$$

with $\rho_{sum} = (\rho_p + \rho_n)$.

To analyze the thermal behavior of a heat flux sensor, we use a simple 1-dimensional model as illustrated in Fig. 2.

We assume that $\lambda_n = \lambda_p = \lambda_{TC}$ and $\lambda_{TC} = \lambda_{Substrate}$. In this model, the effective thermal resistance is given by the resistance of the thermocouple leg

$$R_{th}' = \frac{l}{\lambda_{TC}}. \qquad (8)$$

With these assumptions and eq. (2), the output voltage of the sensor is

$$U = N \cdot \alpha_{pn} \cdot q \cdot \frac{l}{\lambda_{TC}} \qquad (9)$$

and the generated noise voltage

$$U_{ns} = \sqrt{4 \cdot k \cdot T \cdot N \cdot \frac{l}{A_{TC}} \cdot \rho_{sum} \cdot \Delta f} . \qquad (10)$$
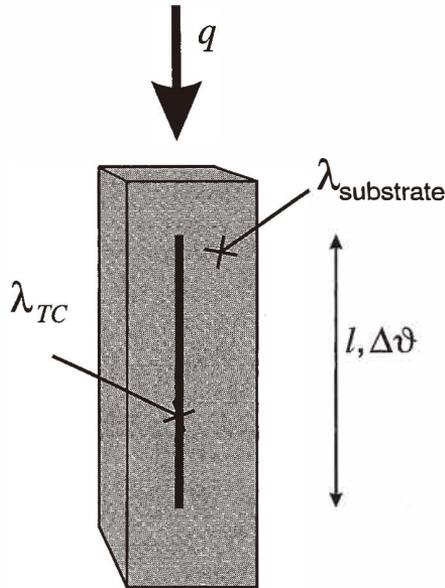
Fig. 2.   Thermoelectric leg.

This leads to a signal-to-noise ratio SNR of

$$SNR = \frac{U}{U_{ns}} = q \cdot \frac{\alpha_{pn}}{\lambda_{TC} \cdot \sqrt{\rho_{sum}}} \cdot \sqrt{\frac{N \cdot l \cdot A_{TC}}{4 \cdot k \cdot T \cdot \Delta f}}. \tag{11}$$

Finally, the noise equivalent heat flux NEHF is:

$$NEHF = \frac{\lambda_{TC} \sqrt{\rho_{sum}}}{\alpha_{pn}} \cdot \sqrt{\frac{4 \cdot k \cdot T \cdot \Delta f}{N \cdot l \cdot A_{TC}}}. \tag{12}$$

From eq. (11), it is clear that the material figure of merit to be maximized is

$$Z_{Sensor} = \frac{\alpha}{\lambda \cdot \sqrt{\rho_{sum}}} \tag{13}$$

This is in contrast to the definition commonly used in connection with thermoelectric power generation.   A comparison of the material figures of merit Z_{Sensor} of different materials in use in thermoelectric applications is shown in Figs. 3 and 4, using values from
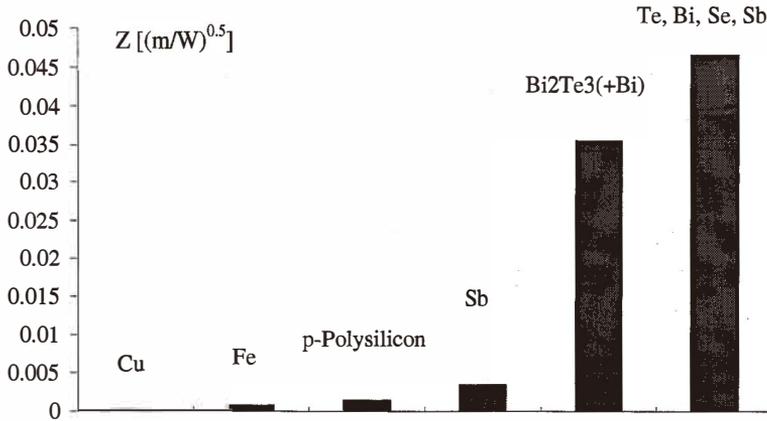
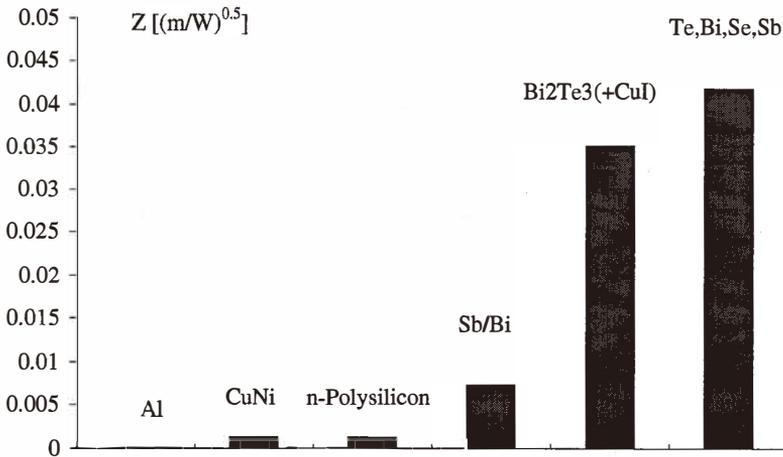Fig. 3.   Thermoelectric materials, p-type.

Fig. 4.   Thermoelectric materials, n-type.

literature at $T = 20/25°C$. The materials from the Bi/Sb/Te group are the most interesting for our purposes; other materials, like polysilicon, which are used in standard CMOS processes, have much lower values. The deposition of thin films of alloys of Bi/Sb/Te, however, is rather complicated.

Therefore, we select 90%Bi-10%Sb as the negative and pure antimony as the positive thermoelectric leg.

3.4 *Geometrical design*

In order to profit from the common methods known from microelectronics, it is of primary importance to create a planar thermocouple structure. Therefore, we disturb the heat flux field in such a way that it induces temperature differences in the plane.

To achieve this, we use the technology of anisotropic silicon etching, known from thermoelectric IR-sensors and other types of sensors:[5] an anisotropic etchant, *e.g.* KOH, has a significantly higher etch rate for (100) crystal planes than for (111) planes. Therefore, it is possible to generate window-like openings in a silicon wafer, protected by a SiO_2 /Si_3N_4 mask (see Figs. 5 and 6).

In this type of design, we have to adapt the thermal analysis of the sensor. For membranes with length much greater than width, the 1-dimensional model illustrated in Fig. 7 holds.[6]

A consideration of the energy balance for a volume element V of the membrane results in the following differential equation for the temperature difference $\Delta T(x) = T_2(x) - T_1$:

$$q = \alpha_{r/c} \cdot \Delta T(x) - \overline{\lambda \cdot d} \frac{\partial^2 T(x)}{\partial x^2} \tag{14}$$

with

$$\alpha_{r/c} = 4 \cdot \sigma \cdot T_0^3 \cdot \varepsilon + \frac{\lambda_{air}}{s}. \tag{15}$$

$\alpha_{r/c}$ is a thermal film coefficient containing a radiation and conduction part; $\overline{\lambda \cdot d}$ is the effective thermal conductivity of the membrane and the thin-film thermocouples (see below); σ is the Boltzmann constant; ε is the emissivity of the membrane; and s is the wafer thickness. The solution of eq. (15) under the obvious boundary conditions is:

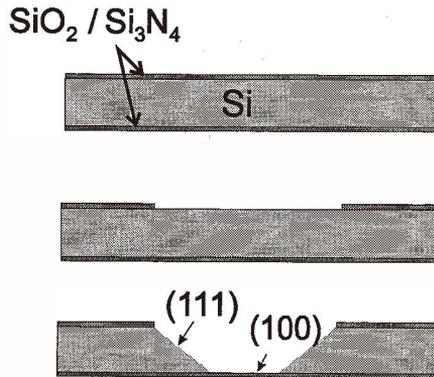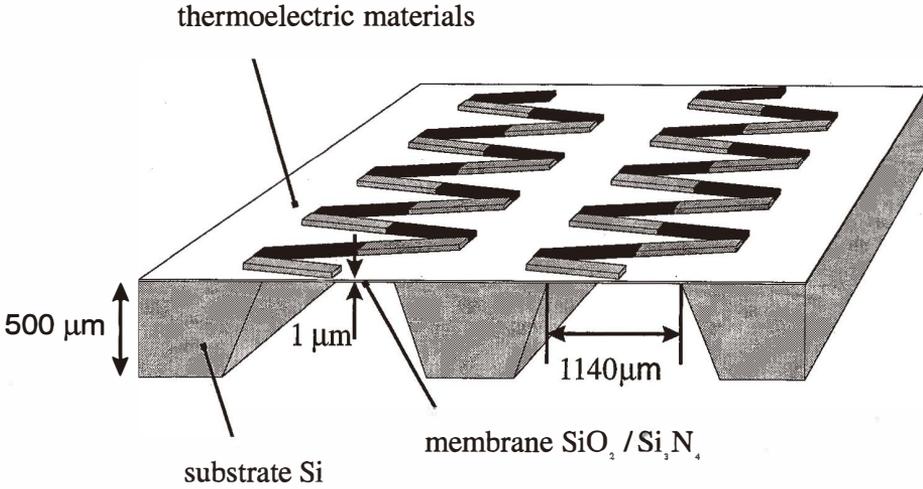Fig. 5.   Anisotropic etching.

thermoelectric materials

Fig. 6.   New design.

$$\Delta T(x) = \frac{q}{\alpha_{\text{r/c}}} \cdot \left(1 - \frac{\cosh(p \cdot x)}{\cosh(p \cdot l)}\right)$$

$$p = \sqrt{\frac{\alpha_{\text{r/c}}}{\overline{\lambda \cdot d}}}.$$

(16)

The temperature difference over the thermocouple is $\Delta T(x = 0)$. To choose a reasonable membrane width, we have to consider the temperature difference over the thermocouple as a function of the length of the thermocouple leg l, $\Delta T(x = 0, l)$

$$\Delta T(x = 0, l) = \frac{q}{\alpha_{\text{r/c}}} \left(1 - \frac{1}{\cosh(pl)}\right).$$

(17)

With our design parameters (thermocouple film thickness: $d_{\text{Bi/Sb}} = 0.5\ \mu\text{m}$, $d_{\text{Sb}} = 0.5\ \mu\text{m}$, $\lambda_{\text{Bi/Sb}} = 4\ \text{W}/(\text{mK})$ $\lambda_{\text{Sb}} = 13\ \text{W}/(\text{mK})$, thermocouple width $w_{\text{Bi/Sb}} = w_{\text{Sb}} = 20\ \mu\text{m}$, thermocouple leg distance $a = 5\ \mu\text{m}$, membrane thermal conductivity λ_{mem}, d_{mem}) and

$$\overline{\lambda \cdot d} = \lambda_{\text{mem}} \cdot d_{\text{mem}} + \frac{2}{5} \cdot \lambda_{\text{Bi}} \cdot d_{\text{Bi}} + \frac{2}{5} \lambda_{\text{Sb}} \cdot d_{\text{Sbi}}$$

(18)

we find the dependence of $1 - 1/\cosh(pl)$ from the length of the thermocouple leg l ($T_0 = 25\text{C}$, $\lambda_{\text{Air}} = 0.026\ \text{W}/(\text{mK})$, $s = 500\ \mu\text{m}$, $\varepsilon = 1$) (Fig. 8).
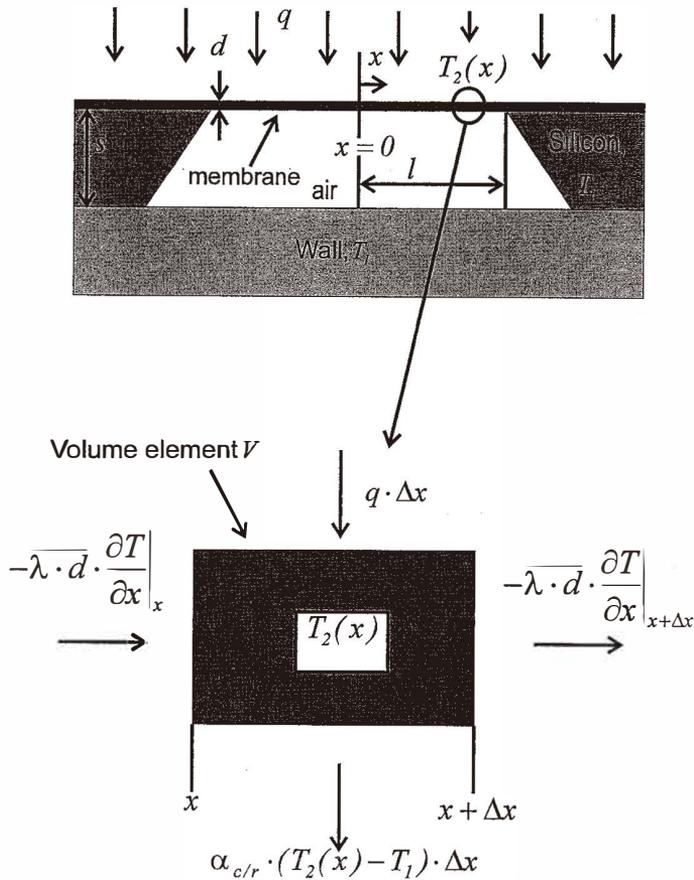
Fig. 7.   Thermal model.

We see that at a length of the thermocouple leg of 570 μm, as in our design, we obtained a temperature difference which is about 70% of the maximum possible value. This result is in good agreement with those which we obtained from 2-dimensional finite-element simulations.

For our measurement purposes, we need a relatively large sensitive area. The dimensions of our nitride/oxide membranes are 1140 μm $\times$ 25000 μm with a thickness of about 1 μm. A sensor contains 10 membranes, each containing 889 thermocouples. The thermocouple array is generated by thermal evaporation of the Bi/Sb-Sb thermocouples. The silicon chip is then bonded on a ceramic substrate of 35 mm $\times$ 35 mm $\times$ 0.254 mm. This results in a total sensor thickness of 0.75 mm. Around the chip, we constructed a ceramic rectangular frame of 0.5 mm thickness (see Fig. 9). A synopsis of the parameters of our sensor is given in Table 1.
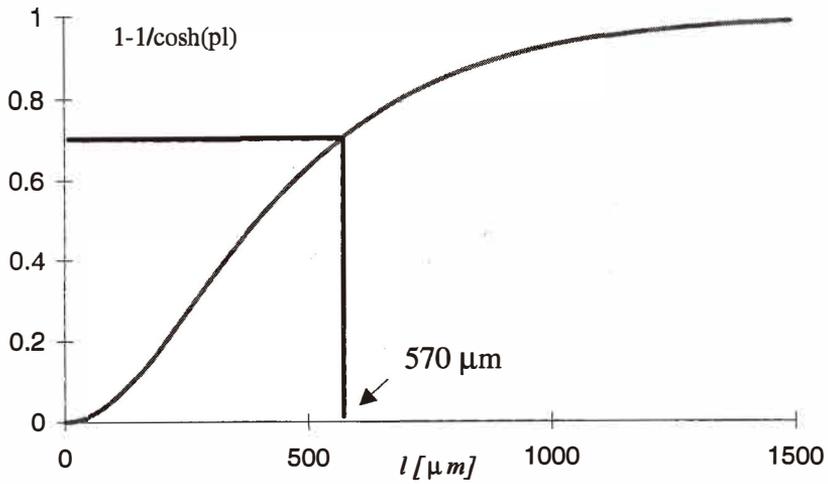
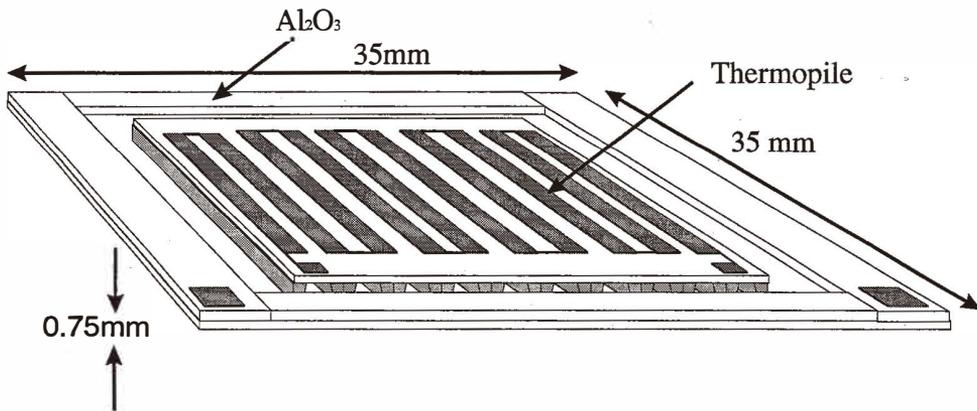Fig. 8.   Temperature difference over thermocouple.

Fig. 9.   Heat flux sensor mounted on ceramic substrate.

4.   Comparison with Conventional Heat Flux Sensors

In Table 2 we show a comparison of the characteristic constants of our sensor with those of commercially available heat flux sensors.

Table 1
Synopsis of sensor parameters.

Active area	[cm^2]	5.55
Film thickness Bi/Sb	[μm]	0.5
Film thickness Sb	[μm]	0.5
Thermocouple length	[μm]	1140
Thermocouple width	[μm]	20
Number of thermocouples	[–]	8890
Responsivity	[V/W]	20 ± 2
Sensitivity	[μV/(W/m^2)]	11000 ± 1100
Resistance	[MΩ]	8 ± 1

5.   Discussion

Our new heat flux sensor is the first which takes full advantage of modern microtechnological developments. Using these fabrication techniques we have managed to improve the responsivity by almost two orders of magnitude and the quality number Q is increased by several orders of magnitude.

In a further step, we will coat our sensors to make them selective for different heat transfer mechanisms: convection, thermal infrared and short wavelengths. This will allow us to measure each of these mechanisms separately at the same location.

Table 2
Comparison with other commercially available heat flux sensors.

		TNO, PU 1.1	Isover St. Gobain	CSEM	ETH Prototype 1
Active area	[cm^2]	1	100	209	**2.2$^{(*)}$**
Thickness	[mm]	3	0.8	~0.5	**0.75**
Thermal resistance	[m^{2}K/W]	1.5×10^{-2}	4×10^{-3}	2.5×10^{-3}	**1.6×10^{-5}**
Density of thermocouples	[cm^{-2}]	?	2	30	**1,600**
Responsivity	[V/W]	0.2	0.0012 – 0.0015	0.001	**20 ± 2**
Sensitivity	[μV/(W/m^2)]	50	12–15	20	**4,400 ± 450**
Quality number	[V^2/(m^{3}KW)]	**8.8×10^2**	**0.7**	**0.8**	**3.3×10^{10}**
Price	[DM]	550.–	600.–	?	**~ 300.–**

(*) partially defective

Acknowledgment

References

1   M. Degree and S. Klarsfeld: A New Type of Heat Flowmeter for Application and Study of Insulation and Systems in Building Applications of Heat Flux Transducers, ed. E. Bales, M. Bomberg and G. E. Courville (ASTM, Philadelphia, 1985) p. 163.
2   Y. Miyake and U. Eguchi: Development of a Large Area Heat Flow Meter in Guarded Hot Plate and Heat Flux Meter Methodology, ed. C. J. Shirtliffe and R. P. Tye, (ASTM, Philadelphia, 1985) p. 171.
3   F. van der Graaf: Heat-flux sensors, in Sensors, Volume 4: Thermal Sensors, ed. T. Ricolfi and J. Scholz (VCH, Weinheim 1992), Chap. 8.
4   F. Porret: Capteurs fluxmétrique de chaleur en technologie couches minces, Rapport Final, Centre Suisse d'Electronique et de Microtechnique S. A. (1986).
5   F. Völklein and W. Schnelle: Sensors and Materials **3** (1991) 41
6   F. Völklein: private communication.